COMPUTATIONAL FRAMEWORK FOR DYNAMIC LOADS ANALYSIS OF THE JOBY EVTOL AIRCRAFT

Michele Castellani*, Sean P. Kelley

**Staff Loads & Aeroelasticity Engineer*
Joby Aviation,
Santa Cruz, CA
USA

ABSTRACT

This abstract presents a computational framework for the dynamic loads analysis of the eVTOL aircraft, developed by Joby Aviation and utilized for the development and certification of the Joby JAS4-1. The novel design features of eVTOL configurations mean that industry-standard methods for loads and aeroservoelasticity, for instance Nastran, lack the modeling capabilities required. Namely, the presence of large wing and tail mounted propellers, whose orientation varies from 0 deg in cruise to 90 deg for VTOL, introduces significant forces and is coupled with the airframe deformation.

The computational framework presented integrates various elements from commonly used methods and tools in structural dynamics and aerodynamics, to build a comprehensive tool that allows performing dynamic loads analyses, such as gust response, landing and oscillatory surface failures.

Specifically, the constitutive elements are

- Structural dynamics: equations of motion based on normal modes, computed by a Global FEM of the airframe (GFEM), built in Nastran.
- Aerodynamics of lifting surfaces: Doublet Lattice Method (DLM).
- Aerodynamics of propellers: propeller force and moment derivatives computed by surrogate model of propeller forces and moments, built via high-fidelity CFD simulations and experimental data.
- Gyroscopic effects of propellers.

The Global FEM of the airframe is built in Nastran, using composite shell elements, 1D elements and lumped masses. Wing and tail pylons are modeled via Craig-Bampton technique, starting from a detailed FEM of each pylon, and adding to the generalized basis interface and normal modes of the subcomponent. Then, modal analyses are performed and generalized mass and stiffness matrices and eigenvector matrices are extracted from Nastran. The equations of motion in modal coordinates are

$$M_{hh}\ddot{q_{hh}} + C_{hh}\dot{q_h} + K_{hh}q_h = \Phi^T F_a(q_h, \dot{q_h}) + \Phi^T F_{gust}(w_g) + \Phi^T F_{prop}(q_h, \dot{q_h}) + \Phi^T F_{prop}^{gust}(w_g)$$

Where the right-hand side includes aerodynamic forces due to lifting surfaces, propellers, gust disturbances, all projected onto the modal subspace. The unsteady aerodynamic forces of lifting surfaces come from the Doublet Lattice Method (Nastran), while propeller aerodynamic forces

are introduced via linearized derivatives of forces and moments at the hub with respect to axial and edgewise inflow ratios, μ_z, μ_x,that is

$$F_z = \rho\pi\Omega^2 R^4 C_{F_z}(\mu_z, \mu_x)$$

$$M_z = \rho\pi\Omega^2 R^5 C_{M_z}(\mu_z, \mu_x)$$

These are linearized about the trim point, such as

$$\Delta F_z = \left(\rho\pi\Omega^2 R^4 \frac{\partial C_{F_z}}{\partial \mu_z}\right)\Delta\mu_z + \left(\rho\pi\Omega^2 R^4 \frac{\partial C_{F_z}}{\partial \mu_x}\right)\Delta\mu_x$$

Inflow ratio perturbations are tied to aircraft motion and to structural modes rotations and velocities of the hub nodes and to tilt angle command $\Delta\vartheta$, by

$$\Delta\mu_z = \frac{v_{axial}}{\Omega R} = \frac{V_\infty}{\Omega R}\Phi_x{}^T \frac{\dot{q}_h}{V_\infty} + \frac{-V_\infty}{\Omega^2 R}\Delta\Omega$$

$$\Delta\mu_x = \frac{v_{edge}}{\Omega R} = \frac{V_\infty}{\Omega R}\Phi_{\theta_y}{}^T q_h + \frac{V_\infty}{\Omega R}\Phi_{\theta_z}{}^T \frac{\dot{q}_h}{V_\infty} + \frac{V_\infty}{\Omega R}\Delta\vartheta + \frac{-V_\infty}{\Omega^2 R}\Delta\Omega$$

The above propeller derivatives are calculated by finite difference around a trim point using predictions from a Gaussian Process Regression (GPR) surrogate model of isolated propeller steady hub forces and moments. This surrogate model is built combing CFD simulations and experimental data.

Some results of the analyses performed employing the developed framework are shown hereafter. Gust response to 1-cosine gust is shown in terms of accelerations at the CG, wing tip and tail tip propellers, Figure 1. The wing shear and bending moment, for a critical time step of the response, are plotted in Figure 2. The two curves compare the response with propellers on and off. The case with propellers off is clearly artificial, but it is shown to highlight how significant the effect is on loads because of the distributed propellers and the relative size of these with respect to the wing area.

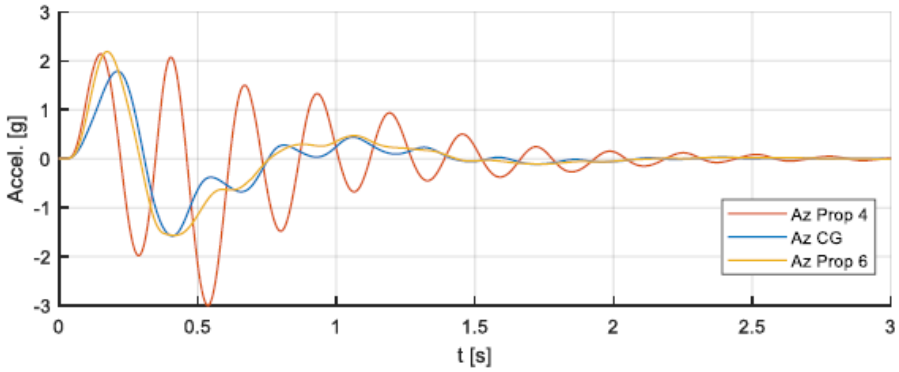

Figure 1: Gust response, accelerations

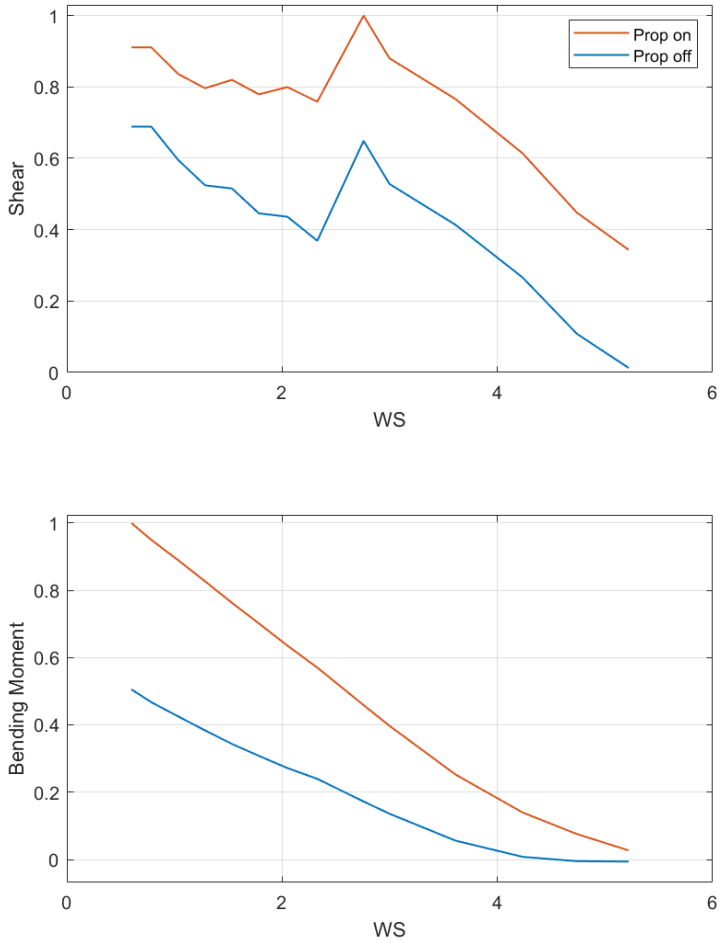

Figure 2: Gust response, wing shear and bending moment